Chapter 1

Introduction

1.1 Background

A new interest in the applications of natural science in an interdisciplinary approach to art and archaeology has prompted the need to look at routine spectroscopic methods that will assist in the study of archaeological samples for identification of underglaze pigments. The results from these studies can be contrasted with those from museum pieces for classification and comparison. These museum pieces are more often than not irreplaceable and therefore necessitate the application of non-destructive methods of analysis to preserve the integrity of these artifacts. The types of art artifacts, among other archaeologically important ones, are paintings, frescoes, paper, leather and – the most resilient artifact that can survive hundreds of years buried in earth and water – porcelain. In recent years there has been a flurry of research activity around the world in various laboratories in search of the most suitable analytical technique, either destructive or non-destructive. Among these are particle-induced X-ray emission (PIXE),[1-3] X-ray powder diffraction, inductively coupled plasma (ICP), optical spectroscopy, atomic absorption spectroscopy (AAS), scanning electron microscopy (SEM)[4,5] and vibrational spectroscopic techniques such as infrared and Raman spectroscopy.[6,7] Although Raman spectroscopy was used to study a number of artifacts, some of which were of archaeological origin, a consistent non-destructive method as applied to the study of underglaze pigments on glazed porcelain was not established. Indeed, Raman spectroscopy was tried for this purpose in other laboratories but due to the high fluorescence emanating from the glaze, it was thought unsuitable for studying underglaze pigments on glazed porcelain.[8,9]

1.2 Statement of the problem

While Raman spectroscopy had been widely used to characterise the glaze on glazed ceramic shards and intact artifacts,[10-15] the ceramic body of broken shards, as well as pigments on broken shards, it had not been successfully used to study underglaze pigments through the glaze on glazed porcelain artifacts (intact or broken shards). However, it had been tried and the frustrations that resulted from repeated attempts to study underglaze pigments on glazed ceramic artifacts non-destructively through the glaze are illustrated by the following excerpts:

> "… *However, the glaze on shards constitute an impediment to analysis by Raman microscopy; such samples were placed for analysis on the XY translation stage of the microscope using a holder which permitted adjustments by rotation about an axis perpendicular to the light beam. In this way the cross-sections of the glazed shards, i.e. the broken edges, could be studied by looking at the coloured layer coating the ceramic material* …".[8,9]

> "… *The major problem which seems to prevent the successful recording of the Raman spectra of underglaze pigments through the glaze itself is the fluorescence under visible excitation …".*[10]

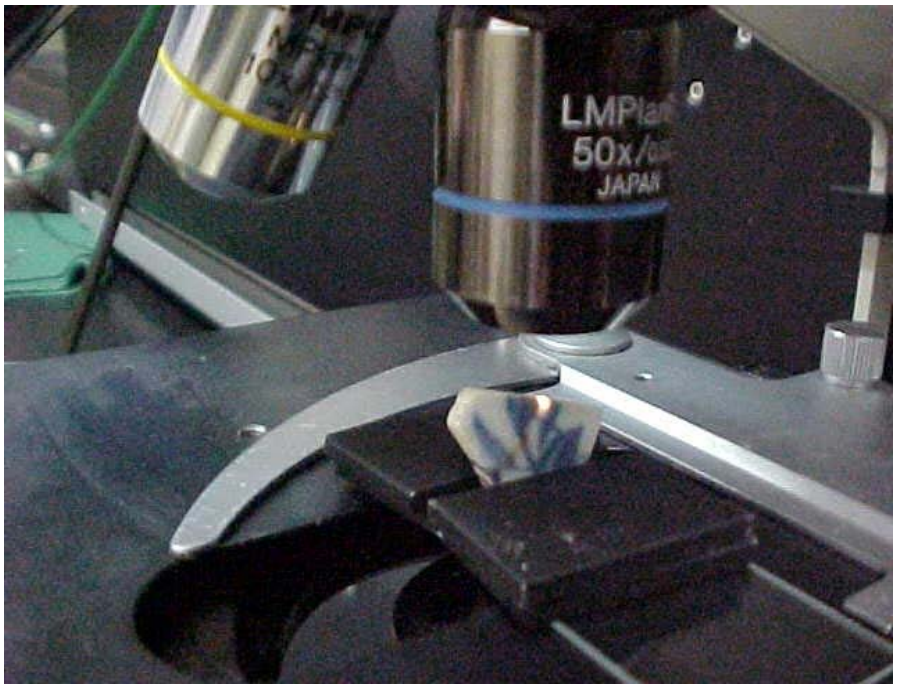

Figure 1.2.1. Due to the inability of researchers to access the pigment of glazed artifacts through the glaze, a shard was often placed in the position shown above in order to access the underglaze pigment on glazed artifacts. This effectively ruled out studies on intact museum pieces where the pigment is not exposed to the surface

Due to the problem presented by the high fluorescence emanating from the glaze of glazed porcelain artifacts, the following solution was developed:

1. Study underglaze pigments on glazed ceramic artifacts on broken edges (as illustrated in Figure 1.2.1.).
2. Study underglaze pigments through the glaze by looking at the influence of fluorescence as impediment.
3. Attempt to extend these methods and present them as routine methods in studying underglaze pigments on glazed porcelain artifacts, both on

broken shards and on intact porcelain artifacts where the pigment is not exposed to the surface for direct study.

4. The result should be applicable to archaeology in order to facilitate the comparison of excavated shards with intact museum pieces on which the pigment is not exposed to the surface for direct study.
5. The results thus obtained should also facilitate the classification and/or identification of the excavated shards in order to assist the archaeologist in correctly identifying and dating the artifact, thereby adding value to the interpretation of findings from historical sites. In some cases the characterisation should be usable in the restoration and preservation of artifacts where applicable.

1.3. Fluorescence: Impediments to the study of underglaze pigments

Fluorescence in Raman spectroscopy as applied to the study of glazed ceramic artifacts greatly affects the spectral assignment because it can mask spectra collected from the glaze and/or pigments in the sample. In the case of glazed ceramic artifacts, the fluorescence emanates from the glaze of the artifact and is attributed largely to the presence of impurities[14] and to the degree of porosity of the glaze under study.[15]

Since the use of a con-focal set-up in Raman microscopy ensures that mainly the spectrum from the focus point is obtained,[16-18] the collection of scattered radiation from volumes in orders of magnitude less than one cubic micron (≤1 μm^3) at the focus point allows high spatial resolution at high spectral resolution (≤1 μm)[19] which can be used to access interfacial pigment spectra from the ceramic/glaze interface. However, this technique has not seriously been attempted as shown by the available literature. The interfacial ceramic/glaze region is usually composed of decorative

pigments and other colouring agents which are the main target for study if one is to identify and characterise these pigments through the intervening glaze.[17,18]

1.4. Pigment characterisation

Although the method of accessing pigment spectra from the interfacial (ceramic/glaze) region is the first step, the ability to characterise and correctly identify the resulting spectra is equally important.

The use of pigments on ceramic artifacts in both art and archaeology can be traced back to antiquity.[19] As such the characterisation of these pigments is of major significance in art analysis and can be used for dating, authenticating and restoring works of art and other historically important artifacts.[19] The pigments are usually made up of natural and/or synthetic pigments whose exact chemical composition and degradation products can assist in deciding on the conservation methods to be used.[20] It is also useful to determine cut-off dates for the manufactured pigments on artifacts by determining the date of first use (or manufacture) of the pigments found on the artifacts,[21] if this can be established. Issues of authentication can often be resolved on the basis of knowledge of the methods used by the manufacturers of the artifacts in comparison with the artifact in question.[17] In some instances, knowledge of pigments that are no longer in use is rediscovered.[22-26]

As a further tool in the process of pigment characterisation, pigments are often synthesised in the laboratory for comparison with pigments on archaeological artifacts for positive identification. The specificity of the Raman signal, which comes from the fact that Raman scattering is a function of the three-dimensional location of atoms in space relative to each other in the scattering medium, makes it possible to consider the Raman signal as a “fingerprint” technique for comparison and/or identification with synthesised pigments. One should always be aware, however,

that the environment in which these pigments are located can also change the Raman spectrum. For instance, cobalt blue on the shards as compared with an isolated pigment shows two different spectra that could be due to stresses in the ceramic/glaze interface and experiments have shown that the physico-chemical environment of this pigment can change the peak intensities.[27]

To this end, a number of pigment databases[28-31] are available for the purposes of comparing spectra from various samples and thereby aid in pigment identification. Reviews have also been published in which emphasis is placed on the publication of extensive pigment spectra for reference purposes. The work of Clark and co-workers aptly fits this description.[32-33] It is therefore not necessary in all instances to synthesise pigments in the laboratory for purposes of positive identification.

1.5. Glaze characterisation

An attempt to collect the Raman scattered radiation from the glaze necessitates a knowledge of the glaze through which this signal is to be collected. This, in turn, may assist in generalising the methods to be used for the various types of glaze, based on composition, sintering temperature (glaze/glass transition temperature at the time of manufacture) and other properties, including the microstructure of the glaze, such as its porosity which, in turn, may contribute to the opacity of the glaze.

1.5.1. Glaze type and composition

The predominant glaze type is based on a silicate (SiO_4) network, with various compounds interspersed throughout this network in various patterns of concentration and distribution. This allows further classification based on how much these elements break or strengthen this silicate network.

The second type of glaze is also composed of a silicate network but with a predominant amount of SnO_2 usually added as an opacifier. This type is expected to affect either the scattered radiation from the ceramic/glaze interface or the incident beam into the sample to the ceramic/glaze interfacial region.

1.5.2. Glaze transition temperature

Due to the strengthening and weakening of the glaze silicate network as a result of the various compounds (network formers (Si and Al oxides) and network breakers or flux (Na, K, Ca, Pb oxides)),[34,35] it is possible to determine the approximate glass transition temperature at the time of manufacture and thereby not only determine the level of technology of the manufacturers,[36] but also compare the various archaeological samples with museum pieces for possible similarity of place of origin[14,17,36] or method of manufacture. Comment on the generality of obtaining spectra through such a glaze from the ceramic/glaze interface can also be made by considering the intensity of fluorescence from the glaze.

1.5.3. Glaze microstructure

Since fluorescence is also a function of the general porosity of the glaze,[1] the microstructure of the glaze should also be an indicator of the success or failure of any method that will attempt to direct a beam through a highly refractive and porous glaze to the ceramic/glaze interface. Comment on the porosity of the samples will therefore add immense value to these discussions.

1.6. Conclusion

The intention in Chapter 1 was to give an overview of and background information on the prevailing situation with regard to the stated problem and the solution being sought.

In summary therefore, it became clear that despite the simplified definition of the problem, the field of archaeology has had limited tools at its disposal without an accurate non-destructive method of characterising underglaze pigments on intact ceramic pieces.

Therefore, a non-destructive method of analysis needed to be devised to unlock the vast body of information buried in these artifacts by identifying the underglaze pigments through the glaze. This will open a new chapter in archaeological research.

1.7. References

1. Cheng, H.S., Zhang, Z.Q., Xia, H.N. and Yang F.J. *Nucl. Instrum. Meth*. 2002, B **190**, 488.

2. Cheng, H.S., Zhang Z.Q., Zhang, B. and Yang, F.J. *Nucl. Instrum. Meth*. 2004, B **219**, 16.

3. Lin, E.K., Yu, Y.C., Wang, C.W., Liu, T.Y., Wu, C.M., Chen, K.M. and Lin, S.S. *Nucl. Instrum. Meth*. 1999, **150**, 581.

4. Padeletti, G. and Fermo, P. *Appl. Phys. A: Mater. Sci. Process*. 2003, **77(1)**, 125.

5. Best, S.P. and Clark, R.J.H. *Endeavour*. 1993, **16**, 66.

6. Davey, R., Gordimer, D.J., Singer, B.W. and Spokes, M.J. J. *Raman Spectrosc*. 1994, **25**, 53.

7. Sato, R.K. and McMillan, P.F. *J. Phys. Chem*. 1987, **91**, 3494.

8. Clark, R.J.H. and Curri, L.M. *J. Mol. Struc*. 1998, **440**, 105.

9. Clark, R.J.H. and Gibbs, P.J. *J. Raman Spectrosc*. 1997, **28**, 99.

10. Brooke, C.J., Edwards, H.G.M. and Taits, J.K.F. *J. Raman Spectrosc*.1999, **30**, 429.

11. Colomban, P*. Appl. Phys. A*. 2004, **79**, 167.

12. Welter, N., Schüssler, U. and Kiefer, W. *J. Raman Spectrosc*. 2007, **38**, 113.

13. Colomban, P., Etcheverry, M-P., Asquier, M., Bounichou, M. and Tounié A. *J. Raman Spectrosc*. 2006, **37**, 614.

14. Osticioli, I., Zoppi, A. and Castelluci, M. *J. Raman Spectrosc*. 2006, **37**, 974.

15. Colomban, P. *Mater. Res. Soc. Symp. Proc*. 2005, **852E**, 008.3.1.

16. Huang, P.V. *Vibrational Spectrosc*. 1996, **11**, 17.

17. Kock, L.D. and de Waal, D. *J. Raman Spectrosc*. 2007, **38**, 1480.

18. Kock, L.D. and de Waal, D. *Spectrochim. Acta*. A.2008, **71**, 1348.

19. Colomban, P., Sagon, G. and Faurel, X. *J. Raman Spectrosc*. 2001, **32**, 351.

20. Colomban, P., Milande, V. and Le Bihan, L. *J Raman Spectrosc*. 2004, **55**, 527.

21. Hwa, L-G., Hwang, S-L. and Liu, L-C. J. *Non-crystalline Solids*. 1998, **238**, 193.

22. Turner, W.E.S. and Rooksby, H.P. *Glastestechniche B*. 1959, **32**, 17.

23. Roy, A. and Berrie, B.H. In: *New Lead-based Yellow in the Seventeenth Century; Painting Technique: History, Materials and Studio Practise*. International Institute for Conservation of Historic and Artistic Works. Roy, A. and Smith, P. (Eds), 1998, p 160.

24. Ravaud, E., Rioux, J-P. and Loire, S. *Techne.* 1998, **7**, 99.

25. Dik, J., Hermeus, E., Perchar, R. and Schenk, H. *Archaeometry.* 2005, **47**, 593.

26. Burgio, L., Clark, R.J.H. and Theodoraki, K. *Spectrochimica Acta A*. 2003, **59**, 2371.

27. Colomban, P., Robert, I., Roche, C., Sagon, G. and Milande, V. *Rev. Aecheometrie*. 2004, **28**, 153.

28. www.chem.ucl.ac.uk/resources/raman/; accessed: January 2008.

29. www.minerals.caltech.edu/files/raman/; accessed: January 2008.

30. www.rruff.geo.arizona.edu/rruff/; accessed: January 2008.

31. www.ens-lyon.fr/LST/Raman/index.php; accessed: January 2008.

32. Correia, A.M., Clark, R.J.H., Ribeiro, M.I.M. and Duarte, L.T.S. *J. Raman Spectrosc*. 2007, **38**, 1390.

33. Clark, R.J.H. C.R. *Chimie*. 2002, **5**, 7.

34. Colomban, P. J. *Non-Cryst. Solids*. 2003, **323**, 180.

35. Colomban, P., de Laveaucoupet, R. and Milande, V. *J. Raman Spectrosc*. 2005, **36**, 857.

36. Ricciardi, P., Colomban, P. and Milande, V. *J. Raman Spectrosc*. 2008, **39**, 1113.

CHAPTER 2

Literature review

The literature on the technique of Raman spectroscopy and its various applications since the advent of coherent lasers is extensive. However, applications of Raman spectroscopy to ceramic artifacts, including those of archaeological origin is relatively recent. Indeed, some of the earlier work on the characterisation of ceramic artifacts was not done through the application of Raman spectroscopy at all. Several other techniques, ranging from particle-induced X-ray emission (PIXE),[1-5] which is an elemental analysis technique, have been used to identify fake porcelain.[2] PIXE has also been used in the elemental characterisation of glass, ancient pottery and porcelain of archaeological origin.[3,6] Although non-destructive, especially in the study of precious artifacts, PIXE was nevertheless deemed to be of limited use with regard to molecular recognition. The obvious limitation of looking only at ratios of elements in an artifact is that one would be unable to distinguish among rutile (TiO_2), Brookite (TiO_2) and anatase (TiO_2)[7] – information that is very important in determining, among others, the possible sintering temperatures of the artifact in question.

Other techniques, such as X-ray diffraction, inductively coupled plasma (ICP) and scanning electron microscopy (SEM),[8,9] have also been used in art analysis. Raman spectroscopy, in particular micro-Raman spectroscopy, where a microscope is coupled to the conventional Raman instrument, presents some very useful advantages over elemental techniques[9] and as a result it emerged as the technique of choice for art analysis in general and archaeological artifacts in particular. This characterisation includes looking at pigments on or beneath the glaze of ceramic artifacts of historical importance[10-13] and, in some instances, has been extended to the study of glaze[14] and the ceramic body itself, beginning with ancient unglazed

pottery[15] and ancient glazed Vietnamese porcelain[16] and extending to glazed Chinese Ming porcelain. [17]

In an attempt to build a coherent picture of the vast applications of this technique in art analysis, P. Vandenabeele[18] presented a broad picture of an interdisciplinary group of disciplines from which art is currently drawing benefits.

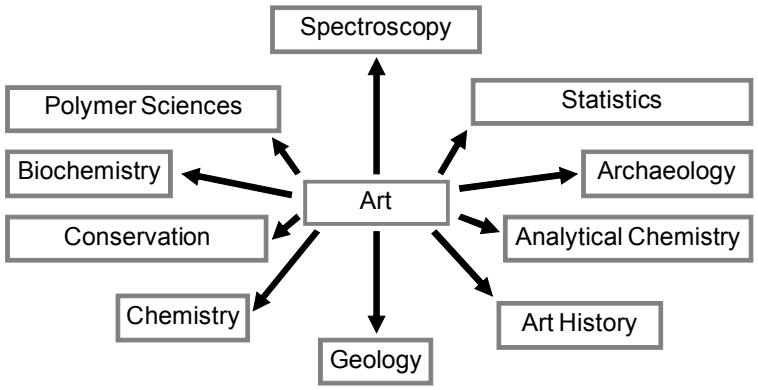

Figure 2.1. Diagram showing the interdisciplinary nature of art analysis and how it relates to a number of research fields (adapted and modified from Vandenabeele[18])

2.1. Studies of glazed blue and white porcelain

In the case of studies of glazed blue and white porcelain, the work of Colomban and co-workers with regard to micro-Raman applications in studying precious ancient glasses, glazes and glass beads using portable and non-portable instruments generated excellent Raman fingerprint spectra of crystalline and glassy phases.[19-22] The portable instruments in some instances produced good results albeit with

difficulty, while laboratory instruments produced excellent results in general. More importantly, however, this work provided information that allowed the researchers to determine the origin and possible date of manufacture of these artifacts where this was in question.

The work of Clark and co-workers, on the other hand, concentrated on ancient pigments (largely inorganic in nature) and their characterisation and identification.[23-26] Many researchers, especially in the early applications of the Raman technique to ceramic artifacts, also reported ceramic body studies together with glaze and/or pigment studies in order to build a coherent picture of the artifact. Examples of these studies include the work of Colomban and his co-workers on Vietnamese blue and white ancient Tham Thai porcelain,[16,19,27,28] as well as the earliest known Meissen porcelain and stoneware.[22] This work also includes studies of ancient Vietnamese porcelain and celadon glazes[29] by these same authors.

Studies by Edwards and co-workers on a porcelain plaque-mounted table[30] and glazed roof tiles[31] can also be considered as examples of the characterisation of ancient ceramics. Several workers in other laboratories have also contributed to this field, including the work of Vandenabeele and co-workers on porcelain cards.[32] Indeed, these authors contributed extensively to the analysis of artifacts using Raman spectroscopy.[33-35] In this section, the literature associated with studies of blue and white porcelain will be reviewed and segmented into three subsections dealing with glaze, pigment and porcelain body, in that order. The emphasis on blue and white is due to the fact that most of the shards in this study are blue and white. There is, however, a tile shard with yellow pigments that has also been included in the study due to differences in glaze type with the blue and white samples.

2.1.1. Glaze composition studies

The literature on glaze composition studies of ceramic artifacts using Raman spectroscopy is new and limited. The glaze on blue and white porcelain shows broad bands around 500 cm^{-1} and 1000 cm^{-1} as reported by Colomban and Treppoz.[36,37] These broad Raman bands are due to the predominance of silicate structure in these types of glaze.[38] However, it was not until recently that Colomban and co-workers developed a method to extract composition information from these broad Raman bands.[39,40]

This method has since been successfully applied to a number of glaze types and also proved useful in not only determining composition, but also processing the temperature of the artifacts at the time of manufacture.[41,42] The composition information on the artifacts has led to the determination of the manufacturing location,[42-44] thus assisting historians and archaeologists in recognising the manufacturing patterns of specific locations.[43,44] Iron Age trade patterns have been studied based on the application of this method to glass beads discovered at archaeological sites in South Africa.[44]

2.1.2. Pigment analysis studies

Throughout the centuries, pigments of various kinds have been used in the decoration of porcelain. With regard to blue and white porcelain artifacts, the most common pigment giving the blue colour is cobalt blue.[45] However, other rare inorganic pigments have been identified on ancient porcelain.[46] Examples of these include lapis lazuli or lazurite ($Na_8[Al_6Si_6O_{24}]S_n$) in 13th century ceramics[46] and more specifically on an Iranian ewer vessel of the 13th century.[47] This pigment was also used in place of the more common cobalt blue on medieval ceramic artifacts from Italy, [48,49] indicating that the blue appearance of archaeological artifacts alone should

not be used to classify these artifacts. Indeed, some researchers contend that lapis lazuli was first used as a pigment as early as 920 AD.[50] Even further back in history, before 3000 BC in Egypt, one finds the use of another blue pigment, called Egyptian blue ($CaCuSi_4O_{10}$), known as "the colour of the eternal sky", which was used to decorate the bust of queen Nefertete who lived during the reign of Pharaoh Akhenaten in Egypt.[51-54] The barium analogue of Egyptian blue, called Han blue ($BaCuSi_4O_{10}$), has also been identified on painted pottery figurines found in Chinese tombs dating from about 1900 years ago.[55] With this in mind, it becomes even more important to identify and characterise correctly any blue pigment found on blue and white ceramic artifacts of archaeological origin.

The literature on blue pigment analysis also places emphasis on the hue of the blue underglaze pigment; it has been shown that the hue of Ming porcelain blue pigment was governed by the amount of manganese added.[55] In some unknown archaeological porcelain samples, however, Raman spectroscopy was used to confirm that amorphous carbon had been added to darken the blue cobalt aluminium oxide.[56] The colour of the blue pigment in the case of the synthesised cobalt blue can also be varied from blue to green by modifying the Co:Al ratio, thereby producing various inverse spinels.[57]

In all these studies involving various types of blue pigment, cobalt blue is the most common pigment responsible for the blue colour and it is clearly distinguishable from the rest by its Raman fingerprint owing to the structure specificity of the Raman technique. Despite this, it was not until recently[58] that its Raman signature on porcelain was recorded and identified.

2.1.3 Porcelain body studies

It is said that long before high-temperature fired Chinese blue and white (transparent) glazed porcelain became popular in Europe, white translucent famous porcelain artifacts had already been produced by Iznik Ottomans.[59] Indeed, the work of Kiefer[60-62] is well known in this regard. This work was further complemented by Henderson,[63] and it was only recently that Colomban and co-workers[64] showed that the white colour of these artifacts actually comes from the α-quartz-rich slip deposited just below the glaze to hide or mask the body which was usually pink/yellowish, as was the case with early Vietnamese porcelain stoneware.[64,65] Colomban and co-workers also showed that the Raman band centre of 500 cm^{-1} related to the lateral displacement of the bridging oxygen (Si-O-Si), whereas the 1000 cm^{-1} Raman band is related to the stretching oxygen (Si-O) vibration. The occurrence of the bands depends on the type of ceramic.[38,66] The Colomban group also identified correlations between processing temperature and raw materials, and these correlations became helpful in using Raman spectroscopy in the study of processing temperature and the material composition of glazes and glass structures. Although the literature on Raman spectroscopy studies of porcelain body composition is very small, detailed Raman spectroscopic studies have been performed on Vietnamese proto porcelain and celadons of the 13th to 16th century[67] and also for the dating of excavated Vietnamese shards and celadons,[68] with good results.

2.2 Pigment analysis on glazed tiles

Glazed tiles are another group of artifacts of historical and archaeological interest. In 1999 post-medieval glazed tiles from Bottesford in Leicestershire, UK, were studied using Fourier Transform (FT) Raman spectroscopy for the first time.[31] Studies on the Bottesford tiles showed that, to a limited extent, some Raman

pigment signature could be obtained through the tile glaze using near-infrared excitation and that fluorescence under visible excitation prevented successful recording of spectra.[31]

Other studies of similar artifacts using Raman spectroscopy include 19th century porcelain cards[32] and an English soft-paste porcelain plaque-mounted table.[30] In both these studies, the pigments that were used for decoration were successfully characterised, except in the case of the blue pigment on the porcelain plaque-mounted table.[30]

2.3. Conclusion

The literature reviewed in this chapter basically shows that the application of Raman spectroscopy in art and archaeology is a very recent field of research. Micro-Raman spectroscopic applications show enormous promise in the study of ceramic/glaze interfacial pigments on porcelain and tiles of archaeological origin. The even narrower subset of this field dealing with applications on blue and white ceramic artifacts of historical and archaeological interest has just begun. Most of the literature is primarily publications of the proof-of-concept type seeking to demonstrate the applicability of Raman spectroscopy in the study of various materials and artifacts. This has been done successfully throughout the literature and the following advantages have been demonstrated:

1. High reproducibility of the Raman spectra
2. High sensitivity (even micro-grains can be studied)
3. Non-destructive (especially important for precious museum artifacts)
4. In situ applications (no sample preparation required)
5. High spatial resolution (≤1 μm^3)
6. High spectral resolution (≤1 cm^{-1})

7. Crystalline and amorphous materials of any colour may be studied

The literature reviewed in this chapter therefore shows a wide area of research opportunity that still remains to be explored, while giving a concise picture of what has already been achieved in the field of Raman spectroscopic studies on blue and white ceramic artifacts of archaeological origin.

2.4 References

1. Cheng, H.S., Zhang, Z.Q., Xia, H.N. and Yang, F.J. *Nucl. Instr. and Meth*. 2002, **B190,** 488.

2. Cheng, H.S., Zhang, Z.Q., Zhang, B. and Yang, F.J. *Nucl. Instr. and Meth.* 2004, **B219,** 16.

3. Cheng, H.S., He, W.Q., Tang, J.Y., Yang, F.J. and Wang, J.H. *Nucl. Instr*. *and Meth.*1996, **B118,** 377.

4. Johansson, T.B., Akelsson, R. and Johansson, S.A.E. *Nucl. Instr*. *and Meth.* 1970, **84,** 141.

5. Johansson, S.A.E. and Johansson, T.B. *Nucl. Instr*. *and Meth.*1976, **137**, 473.

6. Gihwala, D., Jacobsson, L., Peisach, M. and Pineda, C.A. *Nucl. Instr*. *and Meth* 1984, **B3,** 408.; see also Lin, E.K., Wang, C.W., Yu, Y.C., Lin, T.Y., Tan, T.P., Chiou, J.W. and Chin, J. *J. Phys.*1997, **35**, 880.

7. Linda C. Prinsloo, L.C., Wood, N., Loubser, M., Sabine, M.C.V. and Tiley S. *J. Raman Spectrosc.* 2004; **35:** 527.

8. Padeletti, G. and Fermo, P. *Appl. Phys. A: Mater. Sci. Process*. 2003, **77(1),** 125.

9. Best, S.P., Clark, R.J.H. and Withnall, R. *Endeavour.* 1993, **16,** 66.

10. Corset, J., Dhamelin Court, P. and Barbillat, J*. Chem. Br*. 1989, **6,** 12.

11. Clark, R.J.H., Cooksey, C.J., Daniels, M.A.M. and Withnall, R. *Endeavour.*1993, **17,** 191.

12. Clark, R.J.H. *Proc. Int. Conf. on Raman Spectroscopy*, Hong Kong, New York, Wiley, 1994, p 14.

13. Huang, P. V. *Vibrational Spectrosc*. 1996, **11,** 17.

14. MacMillan, B. and Piriou, J. *J. Non-Cryst. Solids*. 1983, **55**, 221.

15. Zuo, J., Wang, C. and Xu, C. *Spectrosc. Lett*. 1998, **31,** 1431.

16. Liem, N.Q., Sagon, G., Quang, V.X., Tan, H.V. and Colomban, P. *J. Raman Spectrosc*. 2000, **31,** 933.

17. Davey, R., Gordimer, D.J., Singer, B.W. and Spokes, M.J. *J Raman Spectrosc*. 1994, **25,** 5318.

18. Vandenabeele, P. *J. Raman Spectrosc*. 2004, **35**, 607.

19. Colomban, P. *Applied Phys. A: Mater. Sci. Process*. 2004, **79,** 167.

20. Colomban, P., Milande, V. and Le Bihan, L. *J. Raman Spectrosc*. 2004, **35**, 527.

21. Colomban, P., Etcheverry, M-P., Asquier, M., Bounichou, M. and Tournié, A. *J. Raman Spectrosc.* 2006, **37**, 614.

22. Colomban, P. and Milande, V. *J. Raman Spectrosc.* 2006, **37**. 606.

23. Correia, A., Clark, R.J.H., Ribeiro, M.I.M. and Duarte, L.T.S. *J. Raman Spectrosc.* 2006, **38**. 1390.

24. Burgio, L. and Clark, R.J.H. *Spectrochim. Acta*. Part A. 2001, **57**, 1491.

25. Clark, R.J.H., *C.R. Chimie*. 2002, **5**, 7.

26. Clark, R.J.H. *J. Mol. Struc*. 2007, **834**, 74.

27. Colomban, P., Sagon, G., Huy, L.Q., Liem, N.Q. and Mazerolles, L. *Archaeometry.* 2004, **46**, 125.

28. Colomban, P., Sagon, G. and Faurel, X. *J. Raman Spectrosc.* 2001, **32**, 351.

29. Liem, N.Q., Thanh, N.T. and Colomban, P. *J. Raman Spectrosc*. 2002, **33**, 287.

30. Edwards, H.G.M., Colomban, P. and Bowden, B. *J. Raman Spectrosc.* 2004, **35**, 656.

31. Brooke, C.J., Edwards, H.G.M. and Tait, J.K.F. *J. Raman Spectrosc.* 1999, **30**, 429.

32. Vandenabeele, P., De Paepe, P. and Moens, L. *J. Raman Spectrosc*. 2008, **39**, 1099.

33. Vandenabeele, P, Edwards, H.G.M. and Moens, L. *Chem. Rev*. 2007, **3**, 675.

34. Vandenabeele, P. *J. Raman Spectrosc*. 2004, **35**, 607.

35. Vandenabeele, P., Bode, S., Alonso, A. and Moens, L. *Spectrochim. Acta*, Part A. 2005, **61**, 2349.

36. Colomban, P. and Treppoz, F. *J. Raman Spectrosc*. 2001, **32**, 93.

37. Colomban, P. *J. Non-Cryst. Solids*. 2003, **322**,180.

38. Liem, N.Q., Thanh, H. and Colomban, P. *J. Raman Spectrosc*. 2002, **33**, 287.

39. Colomban, P., March, G., Mazerolles, L., Karmous, T., Ayed, N., Ennabli, A. and Slim, H. *J. Raman Spectrosc*. 2003, **34**, 205.

40. Colomban, P. In: *Raman Spectroscopy in Archaeology and Art History*, Edwards, H.G.M., Charmers, J.M. (eds). Royal Society of Chemistry, Cambridge, 2004.

41. Colomban, P., Milande, V. and Lucas, H. *J. Raman Spectrosc*. 2004, **35**, 68.

42. Colomban, P., Sagon, G. and Faurel, X. *J. Raman Spectrosc*. 2001, **32**, 351.

43. Colomban, P. *J. Raman Spectrosc*. 2003, **34**, 420.

44. Prinsloo, L.C. and Colomban, P. *J. Raman Spectrosc*. 2008, **39**, 79.

45. De Waal, D. *Asian Chem. Lett*. 2004, **8**, 57.

46. Smith, G.D. and Clark, R.J.H. *J. Archaeol. Sci*. 2004, **31**, 137.

47. Colomban, P. *J. Raman Spectrosc*. 2003, **34**, 420.

48. Clark, R.J.H., Curri, L.M., Henshaw, G.S. and Laganara, C. *J. Raman Spectrosc*. 1997, **28**, 105.

49. Clark, R.J.H., Curri, L.M. and Laganara, C. *Spectrochim. Acta*. 1997, **53**, 597.

50. Brown, K.L. and Clark, R.J.H. *J. Raman Spectrosc*. 2004, **35**, 181.

51. Wiedemann, H-G., Arpagaus, E., Müller, D., Marcolli, C., Weigel, S. and Reller, A. *Thermochim. Acta*. 2002, **382**, 239.

52. Iverson, E. *Dan. Hist. Fild. Medd*. 1955, **34**, 3.

53. Wiedemann, H-G. and Bayer, G. *Anal. Chem*. 1982, **54(A)**, 619.

54. Zuo, J., Zhao, X., Wu, R., Du, G., Xu, C. and Wang, C. *J. Raman Spectrosc*. 2003, **34,** 121.

55. Young, W.J. *Far Eastern Ceram. Bull*. 1949, **8**, 20.

56. Kock, L.D. and de Waal, D. *J. Raman Spectrosc*. 2007, **38**, 1480.

57. Mwenesongole, A. MSc Dissertation, University of Pretoria, 2008.

58. De Waal, D. *J. Raman Spectrosc*. 2004, **35**, 646.

59. Colomban, P., Milande, V. and Le Bihan, L, *J. Raman Spectrosc*. 2004, **35**, 527.

60. Kiefer, W. *Cah. Céram*. 1956, **4**, 15.

61. Kiefer, W. *Bull. Soc. Fr. Céram*.1956, **30**, 3.

62. Kiefer, W. *Bull. Soc. Fr. Céram*.1956, **31**, 17.

63. Henderson, J. In: *The Pottery of Ottoman Turkey*, Y. Petsopoulos, Y. (ed.), London, Alexandria Press, 1989, p 65.

64. Colomban, P. In: *Arts du Vietnam – La Fleur du Pecher et l'Oiseau d' Azur*, Noppe, C., Hubert, J-F. (eds), Tournai, La Renaissance du Livre, 2002, p 100.

65. Colomban, P., Sagon, G., Louhichi, A., Binous, H. and Ayed, N. *Rev. Archaeom*. 2001, **25**, 101.

66. Liem, N.Q., Sagon, G., Quang, V.X., Tan, H.V. and Colomban, P. *J. Raman Spectrosc.* 2000, **31**, 933.

67. Zuo, J., Xu, C., Wang, C. and Yushi, Z. *J. Raman Spectrosc*. 1999, **30**, 1053.

68. Tri, B.M., Tin, T.T., Liem, N.Q. and Colomban, P. *Taoci*. 2001, **2**, 105.

Chapter 3

Synthesis and analysis techniques

The information that is generally sought from studying archaeological samples requires that these samples be studied non-destructively. For this reason, Raman spectroscopy, for its versatility with regard to the wide spectrum of samples that can be studied without any sample preparation, emerges as the single most desirable technique of choice. However, depending on the nature of the sample, it is usually necessary to employ other complementary techniques in order to verify reference samples and/or for use as control techniques for verification purposes. In this work, powder X-ray diffraction (XRD) and energy dispersive X-ray spectrometry (EDX) were used as complementary techniques to the Raman studies. In the following sections, these techniques are discussed, beginning with Raman spectroscopy, followed by X-ray diffraction and concluding with EDX studies.

3.1 Theory of Raman spectroscopy

The Raman Effect was discovered by C.V. Raman in 1927 and the first publication came by way of a letter submitted by C.V. Raman and K.S. Krishnan in *Nature*, 31 March 1928[1]. This discovery was followed by a flurry of papers in which confirmations of Raman's discovery were reported,[2-4] culminating in a review by Pringsheim, in which he labelled Raman's discovery "the Raman Effect".[5] It was, however, not until 1974 that additional intense Raman scattering from pyridine molecules adsorbed at electrochemically roughened silver electrodes[6] was reported, thereby setting off the developments of surface-enhanced Raman spectroscopy (SERS), in addition to normal Raman scattering.[7-9] Today, more than 27 different effects are known as variants of the Raman Effect.[10] These include, but are not limited to, coherent anti-Stokes Raman spectroscopy (CARS),[11] which is well suited

to the study of molecular species in flames, and surface-enhanced resonance Raman scattering (SERRS),[12] a very powerful technique combining the SERS and resonance effects of the Raman technique. There are also novel applications for chiral molecules such as Raman optical activity (ROA),[13] sensitive enough to discriminate between molecular mirror images.

The Raman Effect is basically a scattering phenomenon. When light (monochromatic) is irradiated onto a molecule, the scattered radiation will have the same frequency as the incident radiation (Rayleigh), but will also be accompanied by frequency-shifted radiation on either side of the incident radiation (Stokes and anti-Stokes). This shifted radiation is unique to the scattering media, being dependent on the molecular or crystal structure of the scattering medium.

It is possible to develop a time-dependent quantum mechanical (semi-classical) description of the Raman Effect by considering the phenomenon as a two-photon process.[10,14] However, a classical view also predicts the three types of scattered radiation mentioned above (Rayleigh, Stokes and anti-Stokes). By starting with the equation that relates the electric field ($\vec{E}$) and the induced dipole moment ($\vec{\mu}$) to a first approximation as:

$$\vec{\mu} = \alpha \vec{E} \qquad 3.1$$

where α is the polarisability (second-order tensor). Using the classical electric field equation for $\vec{E}$,

$$\vec{E} = \vec{E}_o \sin 2\pi \nu t \qquad 3.2$$

where $\vec{E}_o$ is the incident electric field, ν is the frequency of the field and *t* is the time defining the evolution of the electric field.

Substituting equation 3.2 into equation 3.1, we obtain the induced dipole moment as a function of the frequency of the incident radiation, ν, and the polarisability, α:

$$\vec{\mu} = \alpha \vec{E}_o \sin 2\pi \nu t \qquad 3.3$$

Because the perturbation of the molecular electron cloud depends on the relative position of the atoms, the polarisability is also a function of the relative position of the constituent atoms.[15] Considering the quantisation of molecular vibrational energy levels, similar to electronic energy levels, the vibrational energy of a particular mode may be written as:

$$\vec{E}_v = (j + ½)h\nu_v \qquad 3.4$$

where j is the vibrational quantum number (j = 0, 1,2,…), ν_v is the frequency of the vibrational mode, and h is the Planck constant. Since the normal coordinate, Q, also varies periodically and is a function of ν_v described in equation 3.4, we can also write

$$Q = Q_o \sin 2\pi \nu_v t \qquad 3.6$$

where Q_o is constant. We also know that in general the polarisability α depends on the molecular normal coordinates Q such that

$$\alpha = \alpha_o + \left(\frac{\partial \alpha}{\partial Q}\right) Q + \cdots \qquad 3.7$$

where α_o is the equilibrium polarisability.

Using equations 3.6 and 3.7 and neglecting the higher-order terms of 3.7, we can write the polarisability α as:

$$\alpha = \alpha_o + \left(\frac{\partial \alpha}{\partial Q}\right) Q_o \sin 2\pi \nu_v t \qquad 3.8$$

and subsequently, the induced dipole moment ($\vec{\mu}$) from equation 3.3 becomes:

$$\vec{\mu} = \alpha_o + \left(\frac{\partial \alpha}{\partial Q}\right) Q_o \sin 2\pi \nu_v t \quad \vec{E}_o \sin 2\pi \nu t \qquad 3.9$$

Simplifying equation 3.7 and using the trigonometric identity:

$$\sin(2\pi \nu_v t) \sin(2\pi \nu t) = \left\{\frac{1}{2} \cos(2\pi \nu_v t - 2\pi \nu t) - \cos(2\pi \nu_v t + 2\pi \nu t)\right\} \qquad 3.10$$

we obtain an equation that contains the difference and sum of the two frequencies (ν and ν_v) of the incident radiation and that of the normal coordinate vibration of the scattering molecule:

$$\vec{\mu} = \alpha_o \vec{E}_o \sin 2\pi \nu t + \frac{1}{2}\left(\frac{\partial \alpha}{\partial Q}\right) Q_o \vec{E}_o \left\{\cos 2\pi\left(\nu - \nu_v\right) t - \cos 2\pi\left(\nu + \nu_v\right) t\right\} \qquad 3.11$$

Inspection of equation 3.11 shows that the induced dipole moment, $\vec{\mu}$, varies with three scattered component frequencies:

1. ν The frequency of the incident radiation (Rayleigh scattering)

2. $\nu - \nu_v$ The incident frequency less the frequency of the normal coordinate vibration (Stokes radiation)
3. $\nu + \nu_v$ The incident frequency plus the frequency of the normal coordinate vibration (anti-Stokes radiation)

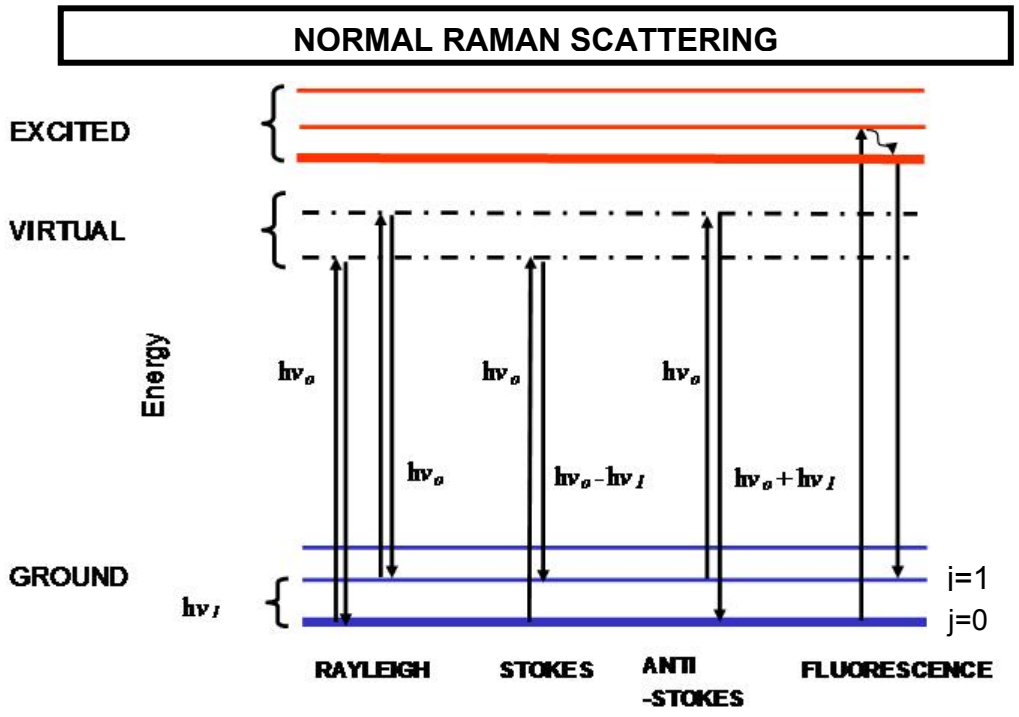

Figure 3.1.1. Illustration of the normal Raman scattering showing Rayleigh, Stokes and anti-Stokes components. The far right depicts fluorescence radiation that, when present, often swamps the Raman signal

Also, looking at equation 3.11, if $\left(\frac{\partial \alpha}{\partial Q}\right)$ is zero and there is no change in the polarisability α with respect to a change in the normal coordinate Q, then there will be no Stokes or anti-Stokes scattering and therefore that particular normal coordinate of vibration will be Raman silent. Clearly, if $\left(\frac{\partial \alpha}{\partial Q}\right) \neq 0$, then the normal coordinate of vibration will be Raman active.

Although the variation of the induced dipole moment with respect to the three types of scattered frequency correctly predicts Rayleigh, Stokes and anti-Stokes radiation, the difference in intensities seen between the Stokes and anti-Stokes radiation emanating from the same normal coordinate of vibration is not predicted by this treatment.

Since the ratio of intensity of the Raman anti-Stokes (L_{AS}) and Stokes (L_S) radiation is predicted to be:

$$\frac{L_{AS}}{L_S} = \left\{ \frac{(\nu_i + \nu_v)}{(\nu_i - \nu_v)} \right\}^4 \exp\left\{ - \left(h\nu / kT \right) \right\} \qquad 3.12$$

where ν_i and ν_v are the incident frequency and the frequency of the normal coordinate vibration, respectively, h is Planck's constant, k is the Boltzmann constant and T is the temperature, then the Boltzmann exponential factor in equation 3.12 guarantees that the anti-Stokes radiation intensity is smaller than the Stokes radiation intensity. Hence a weaker signal from the anti-Stokes radiation is observed when measured.

With reference to Figure 3.1.1., the population of molecules in the $^j = 0$ (energetically most stable) state is larger than that in the $^j = 1$ state. Since the Stokes lines arise from the larger population states ($^j = 0$) of the molecules, the Stokes lines are always stronger than the anti-Stokes lines. It is precisely for this reason that, experimentally, we measure the Stokes rather than the anti-Stokes radiation for easier detection and measurement.

3.2. Applications of the techniques used in the study

This section deals primarily with the various experimental applications of techniques that were used in this study. The major technique, Raman spectroscopy, will be explained first, followed by the complementary techniques of XRD and EDX. The synthesis of reference compounds will also be explained in this section, mainly by way of detailed descriptions of synthetic methods, the results of the syntheses and the purposes for which these compounds were synthesised.

3.2.1. Raman experiments

The Raman experiments were carried out with a Dilor XY multi-channel spectrometer equipped with a liquid-nitrogen-cooled charge coupled device (CCD, model 2000) detector. The system was coupled to an Olympus confocal microscope for the micro studies, with a backscattering (180^{o}) configuration[16] as indicated in Figure 3.2.1.1.

Throughout this work, three types of long-focal-length objective lens (10X, 50X and 100X) were used depending on the sample type and the immediate intent. The 10X objective was used for quick testing and viewing of a sample, while the 50X was used for data collection. The third (100X) was used only in cases where a high degree of spatial resolution and particle discrimination were needed, such as for the detection of mullite in powdered ceramic samples.[16]

Operating conditions included system calibration on a daily basis using the 520.7 cm^{-1} silicon mode. Work proceeded only if this line was within +/- 0.5 cm^{-1} of the silicon line. This procedure is particularly important when changes in closely related Raman band positions are to be discerned. In addition, the day-to-day

consistency of results in Raman band positions is guaranteed. This procedure also enables small shifts in a specific Raman band to be identified.

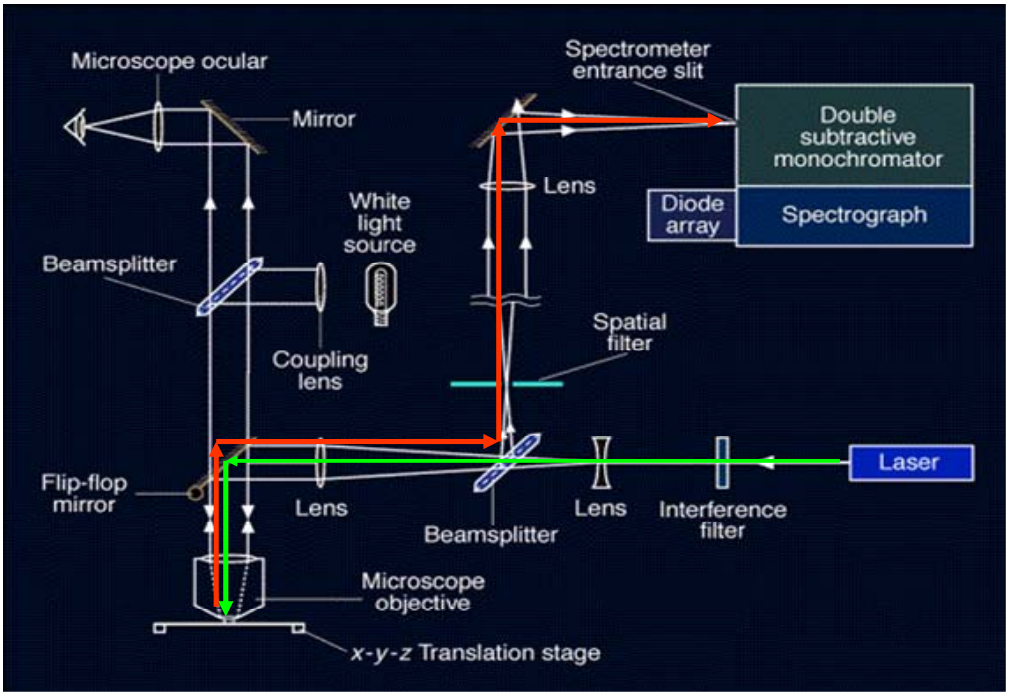

Figure 3.2.1.1. Schematic view of the micro-Raman 180° back-scattering configuration [adapted from: www.ens-lyon.fr/LST/Raman; accessed 20/7/2008]. See also Clark, R.J.H., C. R. *Chimie* 2002, **5**, 7.

The excitation radiation was provided by an Innova 300 Ar^+ laser operating at 514.5 nm wavelength radiation. A Kr^+ laser operating at 568.2 nm wavelength radiation was also used for the Citadel tile studies to observe any excitation frequency dependence of the pigments on the tile. The power outputs of these lasers were optimised to suit the sample under study. For the blue shards, typically between 20 and 40 mW was used, depending on the glaze thickness and whether only a surface spectrum or a ceramic/glaze interface spectrum was acquired. Integration times on blue shards, intact plates and the Citadel tile were typically between 120 and 300 seconds, with three accumulations in each spectral window.

Data acquisition and processing were carried out with Labspec® software version 3.01 provided by Jobyn Yvon of the Horiba group.[17] An Olympus camera (Model Camedia C7070WZ) mounted on top of the microscope was used to acquire the high-resolution pictures. This camera was mounted with an Olympus NFK eyepiece and all the glaze depth profiles were captured with a 50X objective lens on the microscope.

3.2.2. Powder X-ray diffractometry (XRD)

The basic concept of the origin and application of XRD for characterisation purposes is the diffraction of electromagnetic radiation (X-ray) from crystalline solid materials, thereby yielding a diffraction pattern.[18] The resulting diffraction data are then interpreted for purposes of characterising the diffracting material. In this work the powder XRD technique, in which the diffracting sample is composed of randomly oriented crystalline domains, was used. Figure 3.2.2.1 shows a schematic view of an in-phase scattered beam of X-ray radiation.

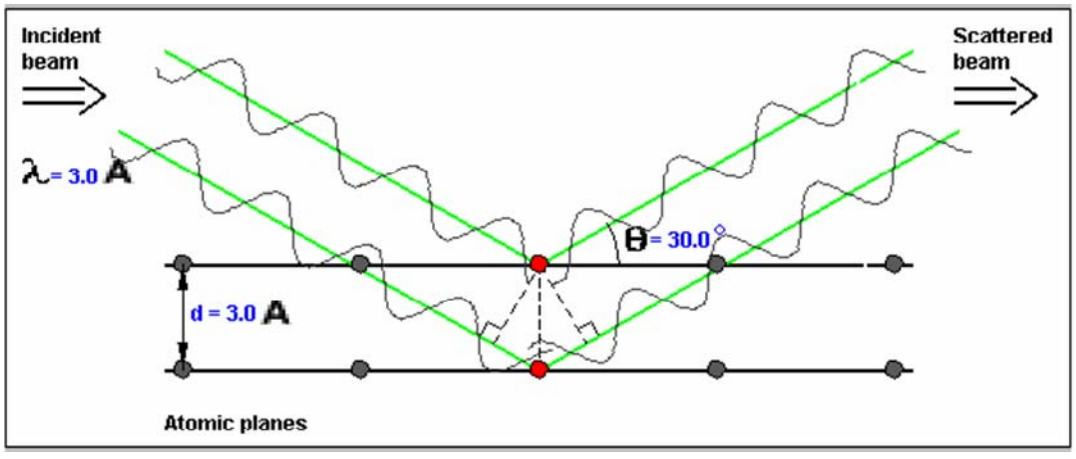

Figure 3.2.2.1. Schematic view of X-ray diffraction from the sample. The scattered radiation contains information on the type and spacing of the atoms in the sample. [adapted from: www.eserc.stonybrook.edu/ProjectJava/Bragg/; accessed 1/4/2009]

This phenomenon, discovered by Sir W.H. Bragg, describes the relationship between the angle, θ, at which a beam of X-rays of wavelength λ can diffract from a crystalline surface given by:

$$2d\sin\theta = n\lambda \qquad 3.13$$

where

λ = wavelength of the X-rays

θ = scattering angle of the beam

n = the order of the diffraction peak.

d = atomic inter-plane distance

Since the detected beam is that for which the Bragg condition was met, information on the inter-plane distance can be obtained from X-ray diffraction experiments. This technique has gone through many technical modifications, leading to very accurate material characterisation techniques using modern instrumentation. The technique of X-ray diffraction is widely applied in material characterisation studies.[19,20] Excellent reviews on X-ray diffraction[21,22] are also available.

Powder XRD studies were used in this study whenever pigment references were synthesised in order to verify the structure and purity of the synthesised compounds. The results of these studies are discussed in the various subsections under Section 4.3 dealing with each pigment. Table 3.2.2.1 shows the data collection parameters from the instrument that was used in all the work done in these studies (at the University of Pretoria's XRD Laboratory).

Table 3.2.2.1. The Instrument and data collection parameters for the Siemens D 501 XRD instrument that was used to collect XRD data on reference samples are given in this table. The samples were prepared using standard Siemens sample holders and the powder was pressed into the holder using a glass slide

Instrument	Siemens D-501
Radiation	Cu Kα (1.5418 D)
Temperature	25 ^{o}C
Specimen	Flat-plate, rotating (30RPM)
Power Setting	40 kV, 40 mA
Monochromator	Secondary, graphite
Detector	Scintilation counter
Range of 2θ	20-70X10^{22}
Step width	0.04X10^{22}
Time per step	1.5 s

3.2.3. Energy dispersive X-ray spectrometry

EDX was used to obtain elemental ratios on the surface. The depth of penetration of the surface in determining selected element ratios was not more that 20 μm. Various positions were selected per sample in order to obtain representative atom ratios.

A JEOL JSM-5800LV model scanning electron microscope was used for the measurements. Since for these types of study a conductive surface is required, gold sputtering on the surface is usually used in the absence of an ultra-high vacuum. However, in this case, since a high vacuum was used, it was not necessary also to use gold sputtering to provide a conducting medium. The recorded range of

between 1.3 and 1.6 for X^2 square values for all EDX measurements in this study was considered to be within the norm.

3.3. Synthesis of selected reference compounds

The following subsections deal with the synthesis of selected reference compounds. These compounds were selected according to the need for verification purposes and were synthesised according to standard literature methods where available. They were analysed using XRD, EDX and Raman spectroscopy. The results are compared and contrasted with those of the pigments identified on the samples under study for positive sample pigment identification and characterisation.

3.3.1. Cobalt aluminium oxide or cobalt blue ($CoAl_2O_4$)

Cobalt aluminium oxide was synthesised in a high-temperature furnace (1 400 ^oC). The method used for this purpose involved using research-grade starting materials (Merck). Two identical samples were treated as follows: cobalt oxide ($CoSO_4$) was intimately mixed with stoichiometric amounts of $Al_2(SO_4)_3$ and dried in the furnace for three hours. The mixture was then fired at 1 000 ^oC for 24 hours in an alumina crucible.[23] At the end of the 24 hours, the furnace was turned off and one of the samples (Figure 3.3.1.1.(a)) was quenched rapidly, while the other sample (Figure 3.3.1.1.(b)) was left in the furnace and allowed to cool slowly to room temperature in the furnace. Figure 3.3.1.1. shows the Raman spectra of the two cobalt blue samples that were prepared and Figure 3.3.1.2. shows the XRD patterns of the final products.

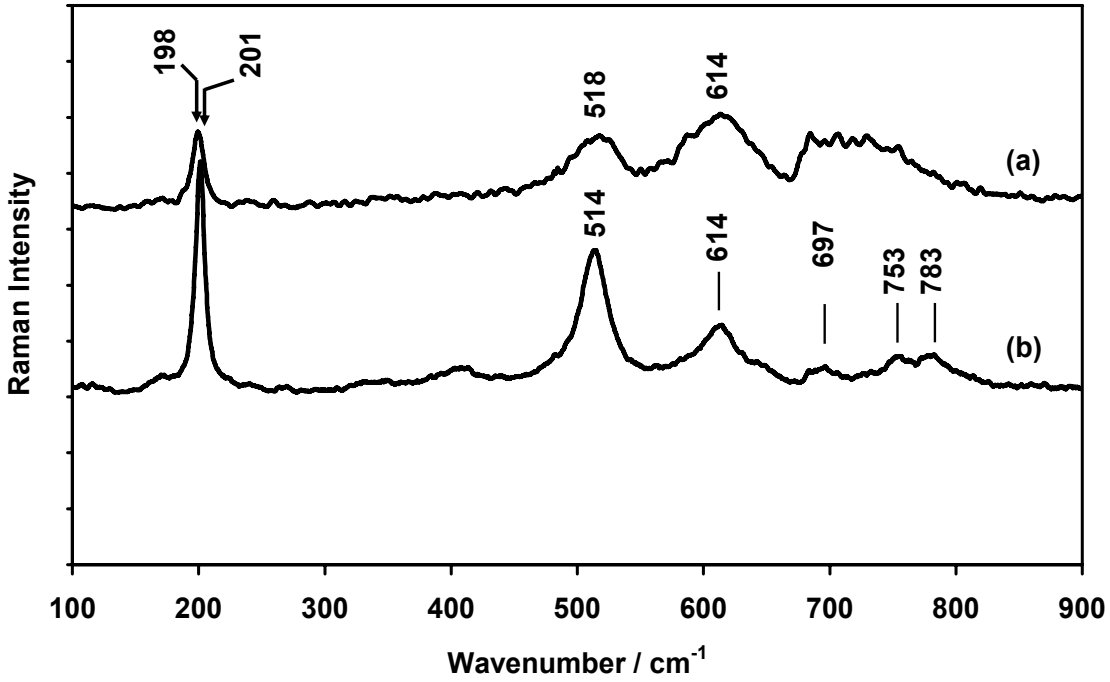

Figure 3.3.1.1. (a-b). Raman spectra of two samples of cobalt blue that were cooled at different rates: (a) cooled slowly and (b) cooled rapidly, at a wavenumber resolution of 2 cm^{-1}.

There seemed to be no difference between the two methods of cooling in the XRD patterns of the cobalt blue samples. However, a slightly less intense Raman band at 198 cm^{-1} was present for the slowly cooled samples. For the rapidly cooled batch it appears at 201 cm^{-1}.

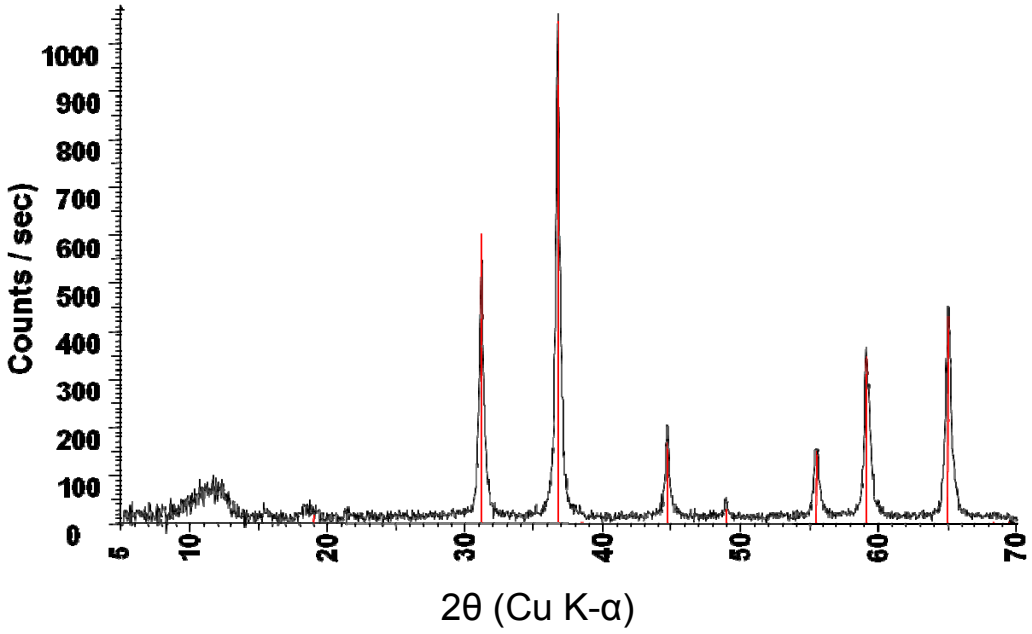

Figure 3.3.1.2. The XRD pattern in this figure is representative of the cobalt blue samples that were cooled rapidly by immediate removal from the furnace.

This same Raman band appears at 195 cm^{-1} on the porcelain shards, which, it is assumed, may have been left in the kiln for slow cooling over several days.[24] However, there are still other differences between the cobalt blue on the porcelain shards and the synthesised free pigment. This will be discussed in Section 4.3.1.

3.3.2. Ternary (Pb-Sn-Sb) oxide ($Pb_2SnSbO_{6.5}$)

For the preparation of the ternary pyrochlore system, $Pb_2SnSbO_{6.5}$, the methods employed by Cascale and co-workers[25] were followed as closely as possible. Stoichiometric mixtures of Pb, Sn and Sb in the form of PbO, SnO_2 and Sb_2O_3 obtained from Merck Chemicals[26] were thoroughly mixed in an alumina crucible and fired in a high-temperature furnace at a temperature of 900 ^oC for 24 hours.

The furnace was then turned off and the products were allowed to cool to room temperature within twenty four hours before XRD and Raman studies could be undertaken. Several samples were prepared in which the ratio Pb:Sn:Sb was varied. Table 3.3.1.2 shows the different samples and the various elemental ratios during preparation.

Table 3.3.2.1. The various samples that were prepared for the purpose of identifying the pigments on the Citadel tile

Sample	(a)	(b)	(c)	(d)	(e)
Pb:Sn:Sb Ratio	2:1:1	2:1:2 (Excess:Sb)	2:2:1 (Excess:Sn)	2:1:0 (No Sb)	2:0:1 (No Sn)

3.3.3. Preparation of lead (II) stannate (Pb_2SnO_4).

The preparation of lead (II) stannate, or lead tin yellow type II, followed closely that of Clark and co-workers.[27] Stoichiometric amounts of Pb_3O_4 and SnO_2 were thoroughly mixed and ground into a fine powder. This mixture was then heated to 900 ^oC for three hours in a high-temperature furnace and the resulting powder was left to cool in the furnace after the furnace had been switched off. Reaction equation 3.3.3.1. shows the open-air formation of the product:

$$2Pb_3O_4(s) + 3SnO_2(s) \longrightarrow 3Pb_2SnO_4(s) + O_2(g) \qquad 3.3.3.1.$$

The solid product in reaction equation 3.3.3.1. was then analysed using powder XRD and the results are shown in Figure 3.3.3.1. The Raman spectrum of lead (II) stannate is shown in Figure 3.3.3.2. The strong Raman band 129 cm^{-1} and medium

band at 196 cm^{-1} was deemed sufficient to identify this compound as lead (II) stannate, and this is also consistent with literature assignments.[28,29]

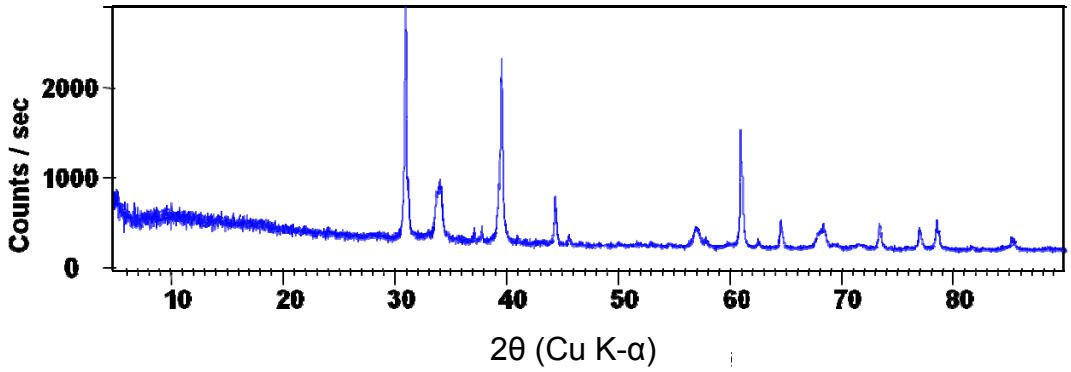

Figure 3.3.3.1. The XRD pattern in this figure is representative of the product in equation 3.1 and has been identified as lead tin yellow type I or lead stannate

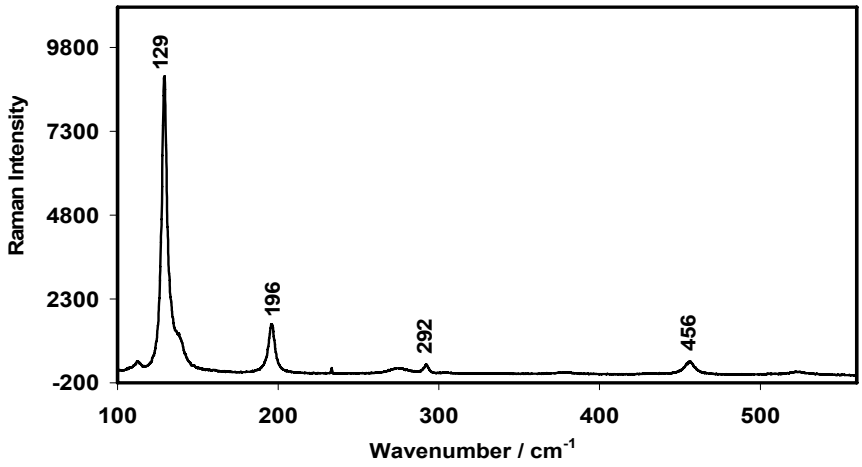

Figure 3.3.3.2. The Raman spectrum of lead (II) stannate (lead tin yellow type I). Incident radiation was 514.5 nm wavelength radiation, with 0.3 mW laser power at the sample. Integration time was 10 seconds and 1 accumulation with wavenumber resolution of 2 cm^{-1}

The results of these analyses were then used in further studies to characterise and identify pigments on the tile shard from the Citadel of Algiers, as discussed in Chapter 5.

3.4. Conclusion

This chapter summarised the techniques that were used in this study (Raman spectroscopy, XRD and EDX). The summary was followed by a description of the synthetic methods that were employed. It was necessary to discuss these aspects in order to clarify the ensuing research, which involved the identification and characterisation of pigments on the blue and white porcelain shards, the intact Ming dynasty plates and the tile shard from the Citadel of Algiers. EDX results for the Citadel tile are discussed in Section 6.2.2.

It is concluded in this chapter that since the field of Raman spectroscopy as applied to samples of archaeological origin is still recent, it is essential that reference compounds are prepared to aid in pigment identification and the building of a coherent body of chemical information for use by archaeologists.

In the case of the blue pigment, differences between porcelain pigment spectra and synthesised references could be investigated as a new line of research. An example would be a detailed study of the structural changes in cobalt blue with changes in pressure, temperature and chemical environment, similar to that found for the ceramic/glaze interfacial region.

The yellow and other pigments on the Citadel tile also presented a unique challenge that required synthesis of reference pigments to aid in the characterization of all the various shades of yellow pigments on the tile. Since the various types of pigments on the tile are lead based, various combinations of Pb,Sn,Sb pigments were

prepared, characterised and comparisons made with results of pigments on the Citadel tile.

3.5 References

1. Raman, C.V. and Krishnan, K.S. *Nature.* 1928, **121**, 501.
2. Rocard, Y. *Comptes Rendus*. 1928, **186**, 1107.
3. Rocard, Y. *Comptes Rendus*. 1928, **186**, 1201.
4. Wood, R.W. *Nature*. 1928, **122**, 349.
5. Pringsheim, P. *Die Naturewissenschaften.* 1928, **16,** 44.
6. Fleischmann, M., Hendra, P.J. and McQuillan, A. *J. Chem. Phys. Lett*. 1974, **26,** 163.
7. Jeanmaire, D.P. and van Duyne, D.P. *J. Electroanal. Chem*. 1977, **84**, 1.
8. Albrecht, M.G. and Creighton, A. *J. Am. Chem. Soc*. 1977, **99**, 5215.
9. Otto, A. In: *Light Scattering in Solids IV,* Cardona, M., Guntherodt, G. (eds), New York, Springer-Verlag, 1984.
10. Long, D.A. *The Raman Effect.* New York, Wiley, 2002.
11. Vestin, F., Afzelius, M., Berger, H., Chaussard, F., Saint-Loup, R. and Bengtsson, P. E. *J. Raman Spectrosc*. 2007, **38**, 963.
12. Carron, K.T. PhD Thesis, Northwestern University, Evanston, Illinois, USA, 1985.
13. Barron, L.D. *Molecular Light Scattering and Optical Activity*, 2nd edition. Cambridge, Cambridge University Press, 2004.
14. Schatz, G.C. and Ratner, M.A. *Quantum Mechanics in Chemistry.* Mineola, New York, Dover Publications, 1993.
15. Colthup, N.B., Daly, L.H. and Wiberley, S.E. *Introduction to Infrared and Raman Spectroscopy*, Academic Press, 1990.
16. Kock, L.D. and de Waal, D. *J. Raman Spectrosc*. 2007, **38**, 1480.

17. Labspec, version 3.01, distributed by Dilor SA and Université de Reims, France, 2004.

18. http://www.eserc.stonybrook.edu/ProjectJava/Bragg/; accessed: April 2009.

19. Ristić, M., Ivanda, M., Popović, S. and Musić, S. *J. Non-Cryst. Solids*, 2002, **303**, 270.

20. Yu, K.N., Xiong, Y., Liu, Y. and Xiong, C. *Phys. Rev. B*, 1997, **55**, 2666.

21. Birks, L.S. *X-ray Spectrochemical Analysis*, 2nd edition. New York, Wiley, 1969.

22. Ebsworth, E.A.V., Rankin, D.W.H. and Cradock, S. *Structural Methods in Inorganic Chemistry.* Oxford, Blackwell Scientific, 1987.

23. King, H.P. and Alexander, L.E. *X-ray Diffraction Procedures*, New York, Wiley, 1954.

24. De Waal, D. *Asian Chem. Lett*. 2004, **8**, 57.

25. Young, J.J. *The Ceramic Art: A Compendium of the History and Manufacture of Pottery and Porcelain*. New York, Harper, 1898.

26. Cascales, C., Alonso, J.A. and Rasines, I. *J. Mater. Sci. Lett*. 1986, **5,** 675.

27. Merck Chemicals, Inc. Johannesburg, South Africa.

28. Clark, R.J.H. *C.R. Chimie*. 2002, **5**, 7.

29. Clark, R.J.H., Cridland, L., Kariuki, B.M., Harris, K.D.M. and Withnall, R.J. *J. Chem. Soc. Dalton Trans*. 1995, **2577**.

30. De Faria, D.L.A., Venancio Silva, S. and de Oliviera, M.T. *J. Raman Spectrosc*. 1997, **28**, 873.